Off-axis dose response characteristics of an amorphous silicon electronic portal imaging device

Peter B. Greer[a)]
Calvary Mater Newcastle Hospital, Newcastle, New South Wales, Australia and University of Newcastle, Newcastle, New South Wales, Australia

(Received 17 April 2007; revised 8 August 2007; accepted for publication 15 August 2007; published 17 September 2007)

Amorphous silicon (*a*-Si) electronic portal imaging devices (EPIDs) have typically been calibrated to dose at central axis (CAX). Division of acquired images by the flood-field (FF) image that corrects for pixel sensitivity variation as well as open field energy-dependent off-axis response variation should result in a flat EPID response over the entire matrix for the same field size. While the beam profile can be reintroduced to the image by an additional correction matrix, the CAX EPID response to dose calibration factor is assumed to apply to all pixels in the detector. The aim of this work was to investigate the dose response of the Varian aS500 amorphous silicon detector across the entire detector area. First it was established that the EPID response across the panel became stable (within ~0.2%) for MU settings greater than ~200 MU. The EPID was then FF calibrated with a high MU setting of ~400 for all subsequent experiments. Whole detector images with varying MU settings from 2–500 were then acquired for two dose rates (300 and 600 MU/min) for 6 MV photons for two EPIDs. The FF corrected EPID response was approximately flat or uniform across the detector for greater than 100 MU delivered (within 0.5%). However, the off-axis EPID response was greater than the CAX response for small MU irradiations, giving a raised EPID profile. Up to 5% increase in response at 20 cm off-axis compared to CAX was found for very small MU settings for one EPID, while it was within 2% for the second (newer) EPID. Off-axis response nonuniformities attributed to detector damage were also found for the older EPID. Similar results were obtained with the EPID at 18 MV energy and operating in asynchronous mode (acquisition not synchronized with beam pulses), however the profiles were flatter and more irregular for the small MU irradiations. By moving the detector laterally and repeating the experiments, the increase in response off-axis was found to depend on the pixel position relative to the beam CAX. When the beam was heavily filtered by a phantom the off-axis response variation was reduced markedly to within 0.5% for all MU settings. Independent measurements of off-axis point doses with ion chamber did not show any change in off-axis factor with MUs. Measurements of beam quality (TMR_{20-10}) for MU settings of 2, 5, and 100 at central axis and at 15 cm off-axis could not explain the effect. The response change is unlikely to be significant for clinical IMRT verification with this imaging/acclerator system where MUs are of the order of 100–300, provided the detector does not exhibit radiation damage artifacts. © *2007 American Association of Physicists in Medicine*. [DOI: 10.1118/1.2779944]

Key words: amorphous silicon, dose verification, EPID

I. INTRODUCTION

Amorphous silicon electron portal imaging devices are currently being utilized for dosimetric verification of intensity modulated radiation therapy (IMRT) fields as well as multileaf collimator and linear accelerator quality assurance. It is therefore important that their dosimetric response characteristics are well understood, particularly the linearity and reproducibility of their dose response.

Generally these characteristics have been assessed for a small detector region at the central axis of the radiotherapy accelerator. Munro and Bouius[1] examined the dose response linearity of a prototype *a*-Si panel with time (dose) from 100 to 3200 ms using a Co-60 beam. They found the response to be linear within 0.14% over this range. El-Mohri *et al.*[2] investigated linearity of a 26×26 cm^2 *a*-Si panel in direct detection mode with a linear curve obtained with doses from 1 to 25 MU. The linearity of the Varian aS500 EPID with increasing MU setting at central axis has been examined by a number of authors.[3–5] The linearity of a newer dosimetric mode that does not exhibit frame loss and acquires extra frames following beam-off to ensure that the final frame is completely read out was examined by van Esch *et al.*[6] They found that the detector had a linear curve for doses from 2 to 300 MU; however, differences below 30 MU were found due to signal rounding. The linearity of the Elekta iView EPID has been examined by McDermott *et al.*[7] and more recently Winkler *et al.*[8] They reported that the reduction in EPID signal for low doses (<15 MU) was due to a dose rate or dose per frame response. They established this by lowering the dose rate (pulse repetition frequency) down to 12 MU/min. For higher doses the detector response also increased more gradually when a uniform dose rate was applied to the EPID. McDermott *et al.*[9] also compared the response of three commercially available EPIDs and found that they all exhibited an increase in response over the initial ~10 MU that was attributed to charge trapping or "ghosting."

These characteristics have been assumed to hold for the entire detector area. However Chin and Lewis[10] found a variation in EPID profiles when the number of frames for the flood-field (FF) and EPID image were varied, with a relatively flat profile obtained for the same number of frames used for each (each acquired image is divided by the FF image). Budgell *et al.*[11] investigated an Elekta *a*-Si EPID for verification of step and shoot intensity modulated radiation therapy (IMRT) verification. They concluded that the device was not suitable for low dose dosimetric QA measurements due to lag/ghosting effects. They found that the EPID profile for a $25\times25\ \mathrm{cm}^2$ field varied in the in-plane direction with monitor unit settings from 1 to 100.

For IMRT applications with the Varian system, there is an initial ramp-up of dose rate in the first 10–20 MU as the beam starts up, and for subsequent segments (change in MLC positions) the linear accelerator either continuously irradiates between segments or "holds-off" beam while the multileaf collimator leaves move to the new position. Therefore changes in beam profile or beam quality that may occur only in the initial dose ramp-up phase would be expected to be less of a problem than other linear accelerator systems that turn the beam on and off for each segment, therefore involving significant dose ramp-up effects.

It has also been determined that *a*-Si EPIDs exhibit a beam energy dependent response that varies with off-axis distance. McCurdy *et al.*[3] investigated with Monte Carlo modelling the central axis response of an *a*-Si EPID to incident beam energy. They found an overresponse at low energies due to the gadolinium oxysulphide phosphor layer. This has a high atomic number and therefore has a greater response per unit incident fluence to low energy photons, particularly below 1 MeV. Kirkby *et al.*[12] measured central axis EPID response to open beams and beams attenuated by compensators. They found the EPID response was reduced for the compensated beams by up to 8% relative to the open beams. The EPID response to off-axis open field radiation has also been found to markedly increase relative to central axis response, with up to 13% at 15 cm off-axis relative to central axis.[13] Differences in EPID response to both open beams and multileaf collimator transmission with off-axis distance have been modelled with Monte Carlo methods.[14,15]

The aim of this work is to examine the uniformity of EPID dose response at both central axis and also over the entire detector relative to the central axis as a function of delivered dose. Large field (whole-detector) images were delivered to two EPIDs for a range of MU settings and the response across the detector assessed at both central axis and at off-axis distances relative to the central axis.

II. METHODS AND MATERIALS

In this work, the linearity of the EPID dose response at the beam central axis with MU setting is first investigated using images acquired with a field size encompassing the entire detector. The response of the EPID at off-axis points relative to the central axis with MU setting was then determined using the same images. To investigate the cause of off-axis variations in EPID response various tests were then performed: (1) Successive identical images were acquired during a long irradiation to examine whether the effects were due to image acquisition time or time from beam start-up, (2) the images were repeated with the EPID offset by 7.5 cm from the central axis in the cross-plane direction to determine if the off-axis response changes depend on the pixel distance from the beam central, (3) measurements were repeated with copper and solid water beam material to determine if filtering the low energy photon component reduced the effects. Finally ion-chamber measurements were made to see whether a change in beam quality at both central axis and off-axis with MU setting could be detected.

II.A. EPID details

All measurements were performed with two aS500 amorphous silicon EPIDs and 21EX accelerators (Varian, Palo Alto, CA), with nominal 6 MV energy photon beams. The EPID was used with 0.5 cm of added perspex buildup to provide charged particle equilibrium at the detector sensitive layer. The buildup was placed on top of the EPID plastic collision cover and completely encompassed the detector. Dose rates of 300 and 600 MU/min were employed. The EPID was operated with continuous frame acquisition during beam delivery. The number of reset frames before image acquisition was zero. The reset frame every 64 frames was removed by a software update. The PV Client software version was 6.1.13 with IAS2 software version 6.1.11. EPID-A was the detector IDU-11 model and was positioned at 105 cm from the source for a dose rate of 300 MU/min and 140 cm from the source for 600 MU/min, while EPID-B was the IDU-20 model and was positioned at 105 cm from the source for all experiments. The EPID image acquisition parameters were for 300 MU/min: Sync mode=4, Rows per PVSync=20, Sync delay=500 ms, and for 600 MU/min: Sync mode=4, Rows per PVSync=9, Sync delay=350 ms. Unless otherwise stated the field sizes used for the measurements were $40\times30\ \mathrm{cm}^2$ for the 105 cm EPID position and $22.5\times30\ \mathrm{cm}^2$ for the 140 cm position.

II.B. EPID dose response measurements

II.B.1. Central axis response

The linearity of the EPID dose-response at the beam central axis was assessed. EPID images were acquired for 6 MV energy at dose rates of 300 and 600 MU/min; for EPID-A from 2 to 200 MU, and for EPID-B for MU settings from 2 to 500. At each MU setting at least three images were acquired to determine the reproducibility. The EPID pixel value was obtained from the reported frame-averaged signal of a 9×9 pixel region at the center of the image, multiplied by the number of frames acquired. The linear accelerator linearity of dose with MU was verified with ion-chamber measurements. A 0.6 cc Farmer-type ionization chamber was aligned with the beam central axis in a solid water phantom at 1.5 cm depth, and 100 cm source-surface distance. The 6 MV beam energy was used with a $30 \times 30\ \mathrm{cm}^2$ field size. Irradiations from 2 to 200 MU were performed with at least three measurements repeated at each MU setting.

II.B.2. Off-axis response

The above images were also utilized to examine the off-axis dose response relative to beam CAX. The EPID was FF calibrated with an approximately 400 MU irradiation prior to the measurements. It was previously determined that the EPID profile was very consistent for MU settings above approximately 200 MU (within 0.2%). The EPID images were all normalized to the beam CAX using the mean of a 9×9 pixel region at the center of each image. Single pixel row profiles from the EPID images were extracted through the central axis in the cross-plane and in-plane directions. These profiles were smoothed with a moving average filter of width 4 pixels.

Ion-chamber measurements were performed to examine whether the beam intensity off-axis relative to central axis was stable with dose. A 0.6 cc Farmer-type ionization chamber was aligned with the beam central axis in a solid water phantom at 1.5 cm depth and 100 cm source-surface distance. The 6 MV beam energy was used with a $30 \times 30\ \mathrm{cm}^2$ field size. Irradiations from 2 to 200 MU were performed with three measurements repeated at each MU setting. The chamber was then moved to 7.5 cm off-axis in the in-plane direction. The readings were repeated for each MU setting at this off-axis position. The ratio of readings off-axis to central axis were taken and compared with varying MU. To determine whether EPID off-axis response effects with MU were reproducible over time, the experimental data set was repeated after a 6 month interval for EPID-B.

II.B.3. Effect of EPID scanning mode on response

The latest version of the EPID, the IAS3 system is set up with a slightly different acquisition parameter set known as asynchronous acquisition for IMRT fields. In this mode the acquisition of image rows is not synchronized with the accelerator beam pulses. This mode is activated by setting the sync mode to zero within the system. In this case the rows per pvsync parameter is not used. The off-axis response images were repeated for EPID-B for 600 MU/min and 6 MV with asynchronous scanning mode for MU settings of 2,5,10, 20, 50, 100, and 200.

II.B.4. Effect of beam energy on response

The measurements for off-axis response outlined above with asynchronous mode were repeated for 18 MV beam energy. No buildup was placed on the EPID, and the EPID was FF calibrated prior to the measurements.

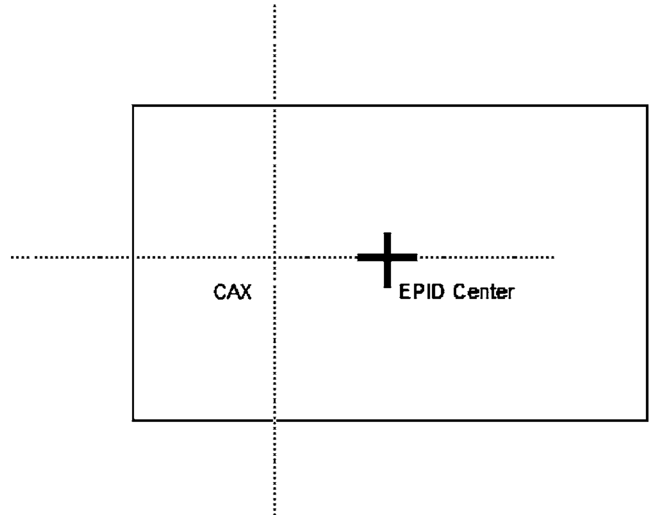

FIG. 1. Diagram illustrating the experimental setup for the offset detector images.

II.C. Investigation of off-axis response

Various methods were used to investigate the off-axis EPID response changes with MU setting.

II.C.1. Movie-loop image acquisition

The variation in EPID images could potentially be due to the detector producing different responses for short images compared to longer images, or could be due to a beam effect where the properties of the beam vary with beam on time. Therefore the image scanning time was fixed and a movie-loop acquisition performed. Successive images were acquired with the $40 \times 30\ \mathrm{cm}^2$ field and EPID-A at 300 MU/min dose rate. A 300 MU irradiation was utilized with 17 images acquired. The image acquisition parameters were identical for these images, with 19 frames acquired for each image (approximately 10 MU per image). The time delay between each image is approximately 2 s due to internal image corrections.

II.C.2. Offset detector

To determine if the off-axis response changes depend on the pixel distance from the beam central axis or from the center of the EPID detector, the images as described in Sec. II B. were repeated with the EPID offset by 7.5 cm from the central axis in the cross-plane direction (Fig. 1). EPID-A was used with the dose rate of 300 MU/min. The field size was not modified from the centered EPID measurements. The EPID electronics lie mainly down the right hand side of the EPID (looking toward the gantry) therefore the EPID was moved to the right so that the electronics were not irradiated by this field. The EPID was first FF calibrated in the offset position with a large ~300 MU setting. An image was acquired with the same MU setting to verify the beam flatness. Images were then acquired with MU settings from 2 to 300. Profiles through the central axis in the cross-plane direction were then extracted.

II.C.3. Spectral filtering

It has been previously shown that the *a*-Si EPIDs overrespond to low energy photon components of the beam compared to ion-chamber.[3] To determine if the off-axis response of the EPID with MU was related to changes in off-axis beam spectrum with beam-on time, filters were used to reduce the low-energy components of the beam. First copper plates were investigated using EPID-B. A 1 cm thick copper layer was placed at the shadow tray level of the accelerator. The images with increasing MU were repeated with the copper in place and compared to those without the copper.

To more strongly filter the beam, the EPID was positioned at 105 cm with the gantry orientated vertically upward. Perspex sheets of 8 cm thickness, and Cu sheets of 1.6 cm thickness were placed on the couch top between the gantry and EPID. The air gap between the filtering material and the EPID was 22.5 cm. This orientation rather than the gantry orientated vertically downward was chosen to allow the largest possible air gap between the filtering material and the EPID while supporting the filter material on the couch top. The field size of 40×30 cm^2 was used at 600 MU/min, with MU settings from 2 to 200. Three images were acquired at each MU setting. The images were all normalized to the 200 MU image. An estimated uniform scatter contribution of 50% was also subtracted from each image.

II.C.4. Beam quality with monitor unit setting

Ion-chamber measurements were made to see whether a change in beam quality at both central axis and off-axis with monitor unit setting could be detected. Measurements of TPR_{20-10} and TMR_{20} were made with a 0.6 cc Farmer-type ionization chamber in a solid water phantom at central axis and 15 cm off-axis. The field was 10×10 cm^2, and readings were made at each depth for monitor unit settings of 2, 5, and 100, to form three sets of TPR values, each set corresponding to a particular MU setting. At least six readings were made for each of the low MU settings to reduce uncertainties.

III. RESULTS

III.A. EPID dose response measurements

III.A.1. Central axis response

Figure 2 shows that the EPID response per MU decreases for low MU settings below ~20 MU with an approximately 3% reduction for the 2 MU setting. This curve is similar to that measured by McDermott *et al.*[9] for the same type of EPID.

The linear accelerator dose per MU was within 0.2% of the 200 MU setting for MUs down to 10 MU and within 0.7% for 5 MU as measured with ion chamber. For the 2 MU setting the dose per MU differed by 1.9% from the 200 MU value. Therefore the MU setting can be taken to be a reliable indication of delivered dose.

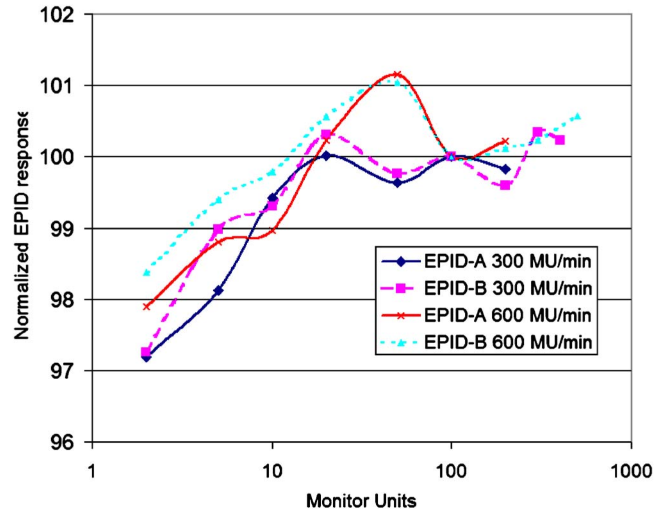

FIG. 2. EPID dose response measured at central axis with MU setting. The response was measured for two EPIDs at dose rates of 300 and 600 MU/min.

III.A.2. Off-axis response

The off-axis response of EPID-A with MU setting is shown in Fig. 3 for 600 MU/min for (a) the crossplane direction and (b) the inplane direction. The results for the EPID-B for 600 MU/min are shown in Fig. 4. All profiles have been normalized to the beam central axis. These show an increase in EPID response at off-axis points relative to the CAX for small MU settings. The response of the EPID becomes relatively stable above approximately 100 MU for both EPIDs. For EPID-B, the newer unit, the profiles show an off-axis change in response that is relatively uniformly increasing with off-axis distance. The results were similar for the two dose rates with a slight increase in the magnitude of the off-axis response for 600 MU/min. For EPID-A, the older detector, the response is more nonuniform with off-axis position, with the cross-plane profiles becoming very noisy at low MU settings and the inplane profiles asymmetric. Both EPIDs show a central "depression region" where the response is relatively flat. This region corresponds approximately to a 10×10 cm^2 field size.

The ratio of readings off-axis to central axis with varying MU as measured by the ion chamber are given in Table I. These show that the beam off-axis ratio is stable with MU settings and is not the cause of the EPID response changes.

The responses for EPID-B measured at 6 month intervals were very similar, within approximately 0.5%. This suggests that these patterns of response are relatively stable over time.

III.A.3. Effect of EPID scanning mode on response

The results for the EPID profile response with asynchronous scanning are shown in Fig. 5. The profiles shown a trend similar to the previous results down to MU settings of approx 20 MU; however, for the images below 10 MU the

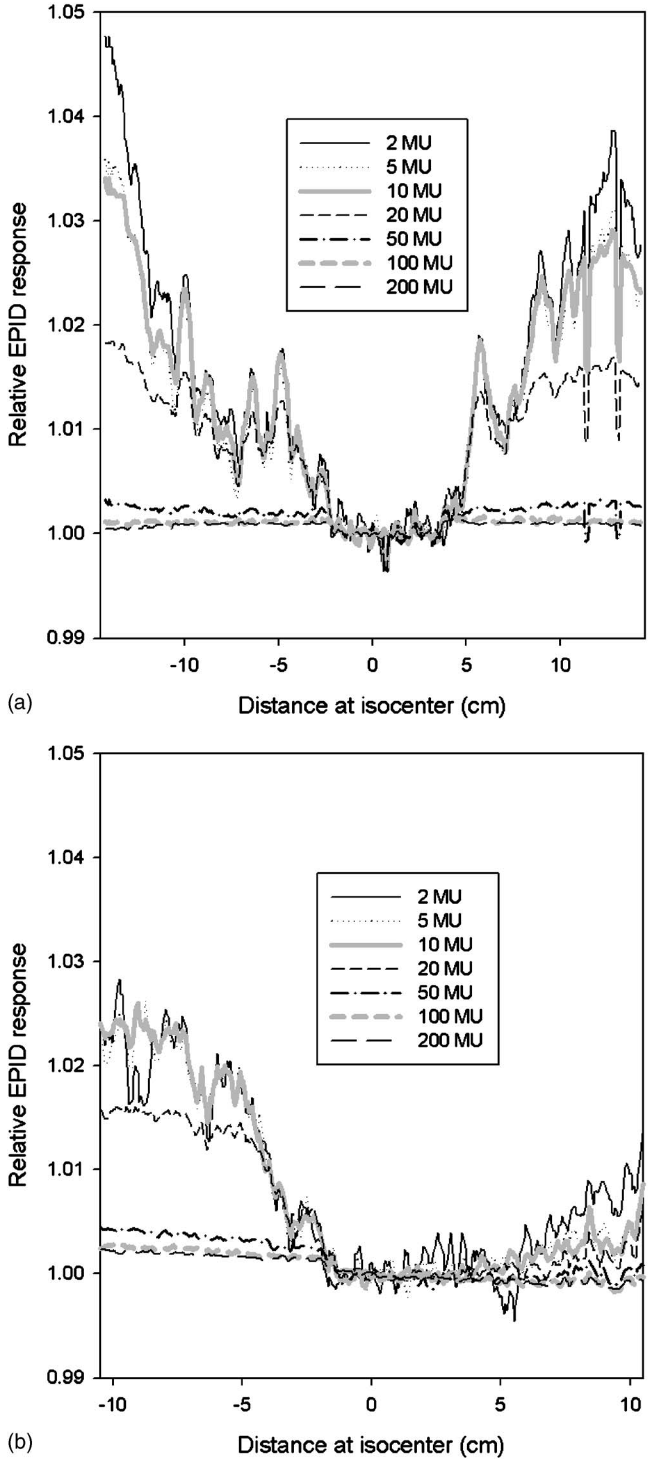

FIG. 3. EPID response relative to central axis with monitor unit setting for EPID-A at 600 MU/min and 6 MV energy for (a) cross-plane direction, and (b) in-plane direction.

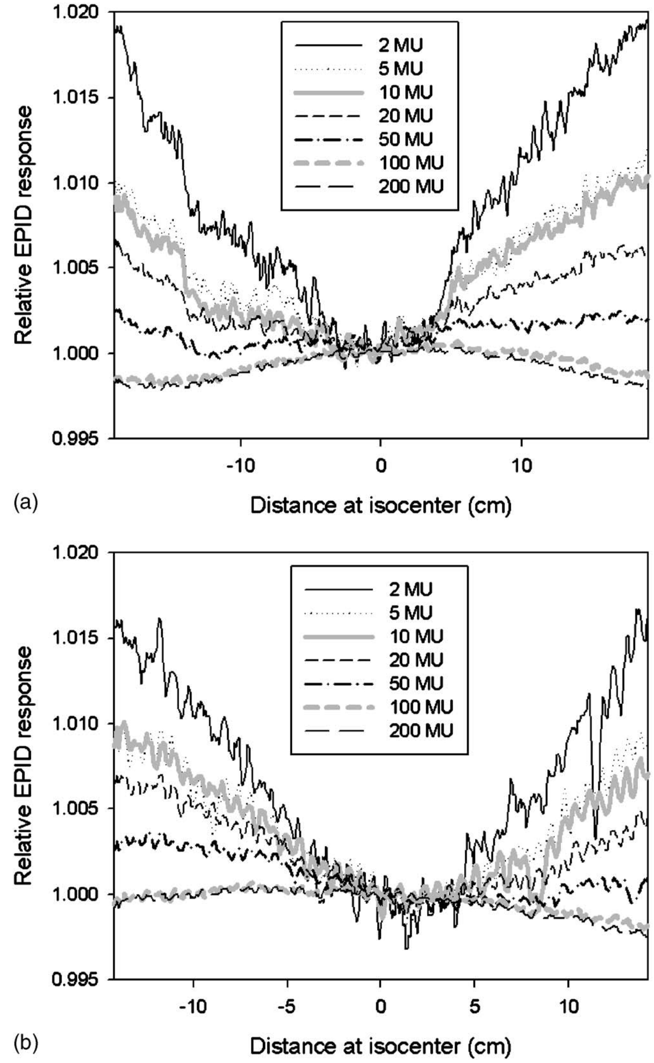

FIG. 4. EPID response relative to central axis with MU setting for EPID-B at 600 MU/min and 6 MV energy for (a) cross-plane direction, and (b) in-plane direction.

EPID profiles were flatter with this mode as well as more irregular, with undulations in the profiles in the in-plane direction.

III.A.4. Effect of beam energy on response

The results for the EPID response for 18 MV energy with asynchronous imaging mode are shown in Fig. 6. Similar trends were observed at 18 MV but with the off-axis response lower at 18 MV compared to 6 MV. For example for EPID-B at 20 MV the 6 MV response is approximately 0.5% higher at 20 cm off-axis than at central axis, whereas at 18 MV this reduced to approximately 0.3%. The EPID re-

TABLE I. Off-axis ratio at 7.5 cm measured with ion chamber as a function of delivered dose (MU). The standard deviation of the ion-chamber measurements at each setting was within 0.3% at central axis and 1.8% at 7.5 cm off-axis.

Monitor Units	Off–axis ratio
2	1.031
5	1.030
10	1.032
20	1.031
50	1.031
100	1.030
200	1.030

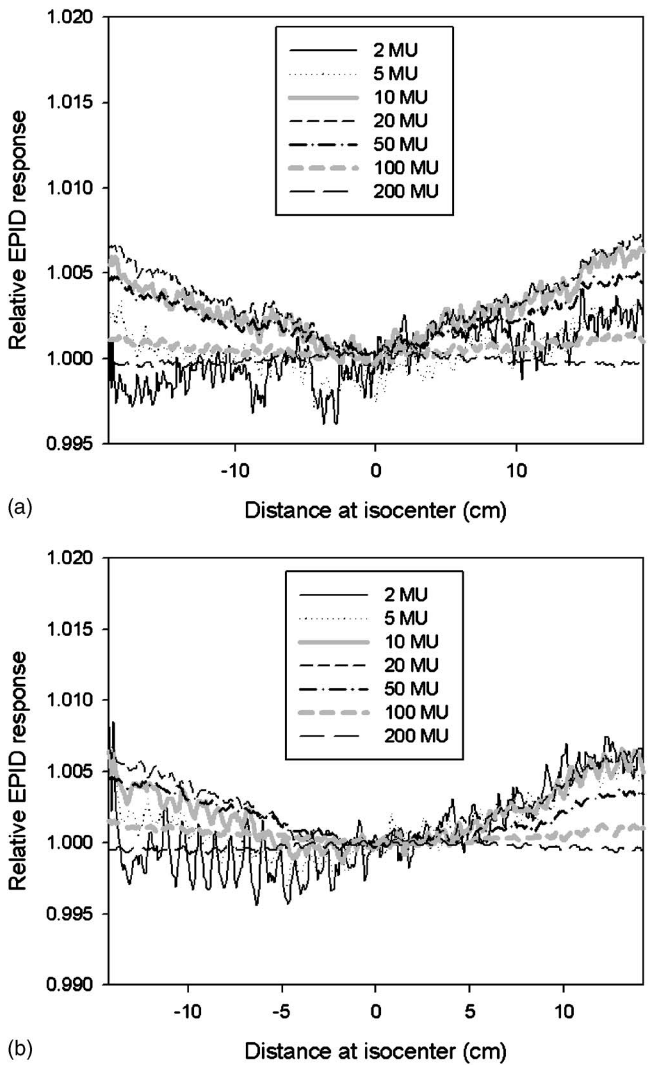

FIG. 5. EPID response relative to central axis with MU setting for EPID-B at 600 MU/min and 6 MV energy with the EPID operating in asynchronous scanning mode for (a) cross-plane direction, and (b) in-plane direction.

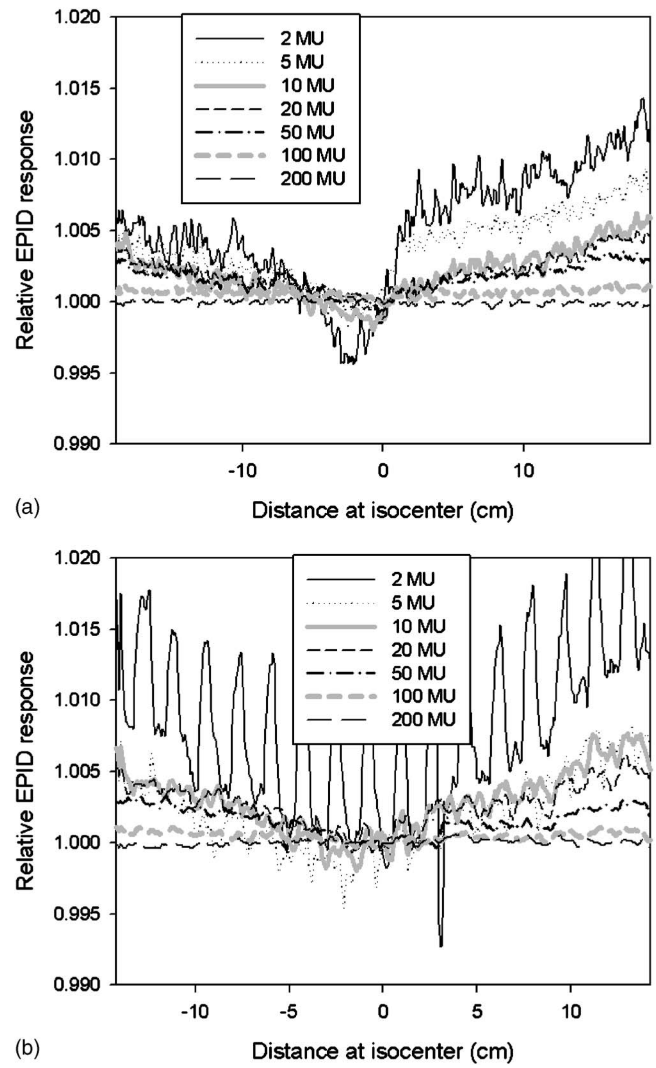

FIG. 6. EPID response relative to central axis with MU setting for EPID-B at 600 MU/min and 18 MV energy with the EPID operating in asynchronous scanning mode for (a) cross-plane direction, and (b) in-plane direction.

sponse becomes highly irregular for the small MU settings, and the undulation increases in the inplane direction.

III.B. Investigation of off-axis response

III.B.1. Movie-loop image acquisition

Figure 7 shows the profiles in the cross-plane direction for the 19 frame movie-loop acquisitions. These profiles show that the images taken at the start of the irradiation exhibit the increase in response off-axis, whereas the images taken at the end of the irradiation are more uniform in response. These results suggest that the effect is related to the time from the initial beam-on, rather than an imager effect related to the number of frames acquired in an image. Each of these image acquisitions were identical, apart from the time from the initial beam-on that they were acquired.

III.B.2. Offset detector

The profiles through the central axis in the cross-plane direction for the EPID offset by 7.5 cm in this direction are shown in Fig. 8. These exhibit a similar increase in EPID response off-axis for the shorter MU irradiations. However, the response is clearly centered about the beam central axis rather than the center of the EPID. This suggests that the EPID response is related to some property of the radiation beam with off-axis distance rather than related to the distance of a pixel from the center of the EPID.

III.B.3. Spectral filtering

Figure 9 shows profiles with the 1 cm Cu filter present at the shadow tray level of the accelerator for EPID-B at 600 MU/min. These can be compared with Fig. 4 acquired without any filtration. These show an apparent reduction in the off-axis response of the EPID when the Cu plate is present. The EPID was FF calibrated with the copper present, in a similar way to the unattenuated results.

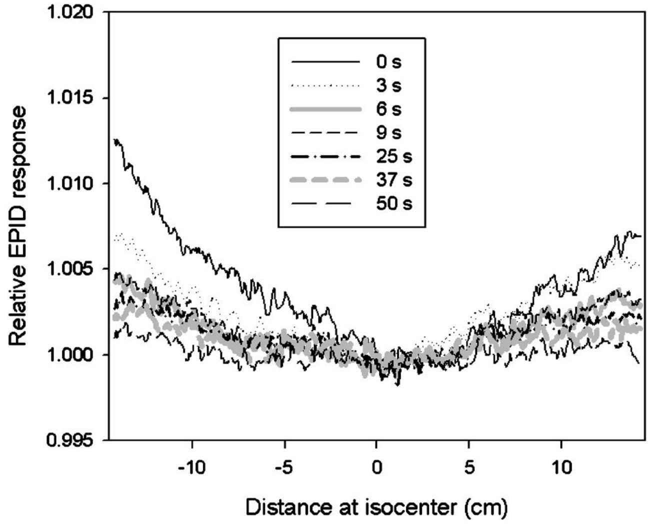

FIG. 7. EPID response in the cross-plane direction for EPID-A for successive 19 frame images, acquired during a long 300 MU irradiation. These are plotted according to the approximate time of the start of each image.

Figure 10 shows the profiles through central axis for the images acquired from 2 to 200 MU with the 8 cm perspex and 1.6 cm of Cu present to filter the beam. These are normalized to the 200 MU field as a FF calibration was not performed. These show a large reduction in the off-axis response with MU.

III.B.4. Beam quality with monitor unit setting

The results for the beam quality TMR_{20} and TPR_{20-10} measurements are given in Table II. A slight increase in beam quality is apparent for the 2 MU settings particularly off-axis, however the values are all equivalent within the experimental uncertainties.

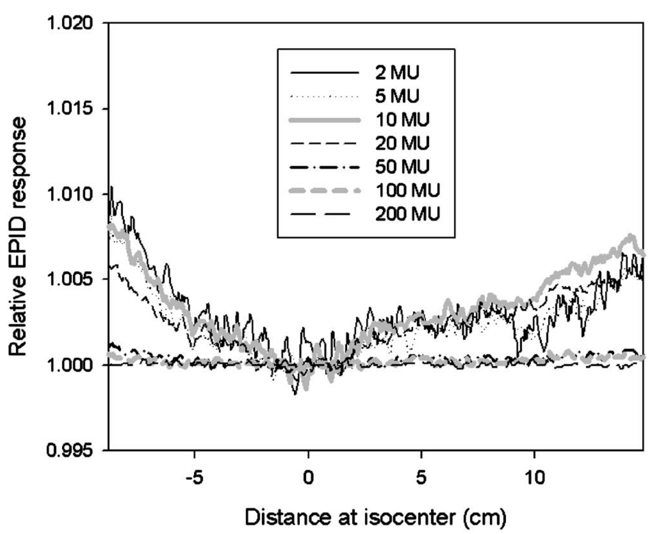

FIG. 8. The response of EPID-A in the cross-plane direction with the EPID detector offset by 7.5 cm in this direction. The distance refers to distance from the central axis of the beam.

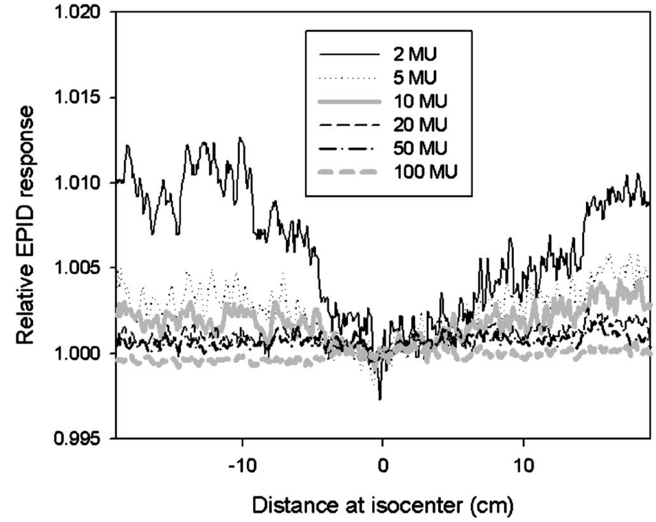

FIG. 9. The response of EPID-B in the cross-plane direction with 1 cm of copper filtration placed on the shadow tray level of the accelerator.

IV. DISCUSSION

The results for central axis EPID dose response are in agreement with previous studies.[8,9] There is a sharp increase in EPID response with increasing MU for the low MU dose range. The response is relatively stable from above 20 MU although a small increase is seen with increasing MU. However measurements for other EPID types have shown a decrease in response of up to 10%. This suggests that the off-axis response effects may be greater for other EPID/linac manufacturers. A greater change in off-axis response with MU for the Elekta EPID is also apparent in the measurements reported by Budgell *et al.*[11] Winkler reported for a different type of *a*-Si EPID that at low doses the increase in response was due to a dose-rate response of the EPID. The dose rate is lower as the beam starts up and rises to the

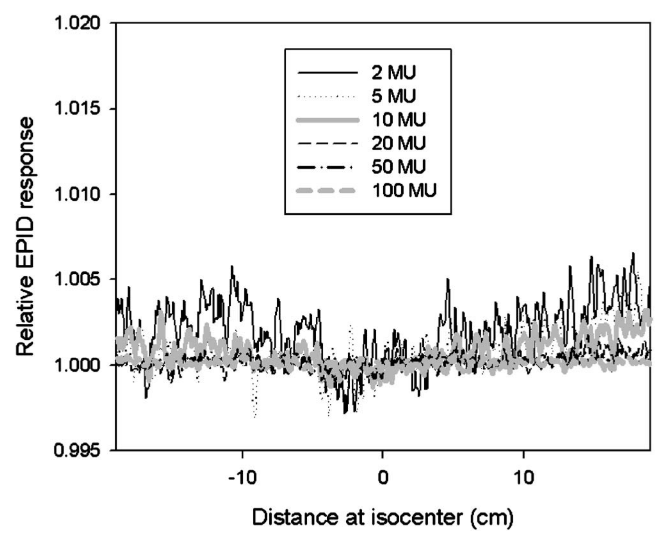

FIG. 10. The EPID response is shown for EPID-B with 8 cm of perspex and 1.6 cm of copper placed between the source and the EPID, with a 22.5 cm air gap. The profiles were normalized to the 200 MU setting image.

TABLE II. Beam quality $TMR_{20\ cm}$ and TPR_{20-10} at central axis and 15 cm off-axis as a function of delivered dose (MU). The uncertainties are given as ±2 standard deviations of the measurements.

Monitor units	TMR_{20} (Central axis)	TMR_{20} (15 cm off-axis)	TPR_{20-10} (Central axis)	TPR_{20-10} (15 cm off-axis)
2	0.523±0.016	0.488±0.005	0.671±0.014	0.643±0.008
5	0.525±0.007	0.483±0.002	0.667±0.009	0.639±0.004
100	0.523±0.000	0.483±0.000	0.666±0.000	0.638±0.000

nominal dose rate, and the EPID response is reduced for the lower dose rate. The increase in response for higher MU settings can be attributed to a "ghosting" or charge-trapping effect. To examine the dose-rate dependence with the Elekta EPID, Winkler *et al.* were able to reduce the pulse repetition frequence of the accelerator to produce dose rates as low as 12 MU/min. It is not possible with the Varian system to lower the dose rate in this manner. The measured dose or MU dependence of the EPID can be incorporated as an additional correction factor for converting EPID response to dose. The results also exhibit a small increase in response at the 600 MU/min dose-rate following the steep increase in response. The reason for this is not clear but could be due to an overshoot in dose rate that occurs at this high dose rate before the dose rate settles at its nominal value.

Experiments were performed to determine if the observed change in EPID off-axis response with MU was due to a dose-rate effect response. The response of the EPID was measured for the six linear-accelerator dose-rate settings of 100 to 600 MU/min. Identical IMRT imaging parameters were set for each imaging mode at each dose rate. FF calibrations for 100 MU each were performed for each mode followed by 10×10 cm^2 images for 100 MU. Mean pixel values in a region of interest of 14×14 pixels at the central axis were examined for both the FFs and the 10×10 cm^2 images. However the results were extremely inconsistent with dose rate, and no conclusions could be drawn.

A second approach was investigated where the dose rate was set to 100 MU/min and the EPID distance from the source was varied from 105 to 182 cm to reduce the dose rate incident on the EPID due to inverse square falloff. A 10×10 cm^2 image for 100 MU for each position was used and the mean pixel values in a region of interest of 14×14 pixels at the central axis was examined. The EPID response at the greatest distance was approximately 5% higher than the response change expected due to inverse square falloff. The gantry was rotated to 270° for these measurements to ensure that backscatter from the floor was not affecting the EPID signal. This is in the opposite direction to the observed reduction in EPID response with reducing dose rate in the literature and clearly requires further investigation. A potential explanation for this is that backscatter from the EPID housing is increasing the EPID response.[16] As the distance from the source increases, the field size at the EPID becomes larger, and more backscatter sources underneath the EPID can contribute to the signal. The possibility that the measured profile effects observed here are due to dose-rate response effects remains open. The instantaneous dose rates off-axis could be different with beam start-up and the addition of filtration material will reduce this difference. The author aims to investigate the dose-rate effects in more detail in further work.

The EPID response increases with off-axis distance relative to central axis with reducing MU setting. Because these EPID images are FF corrected, and were acquired with the same field size as for FF calibration, a completely flat EPID response profile is expected. This is because the profiles in the FF correction image and the acquired image should be the same and therefore cancel. It was found that the EPID profile was very stable (within 0.2%) from 200 MU and higher, and therefore the FFs were acquired with high MU settings of 300–400 MU. This was done so that the FF represented a stable EPID response, and then variations in the acquired EPID image profile could be studied with MU setting.

Chin and Lewis[10] found a variation in EPID profiles when the number of frames for the FF and EPID image were varied, with a relatively flat profile obtained for 211 frames used for each. They found that EPID profiles in the cross-plane direction with a 60 frame FF and image frames of 211 and 835 decreased relative to central axis. These are consistent with the findings here. For example, the 835 frame image will be relatively flat in profile, while the lower 64 frame FF image will have an increasing response with off-axis distance. Therefore the division will result in a FF-corrected image that decreases with off-axis distance. In this work we isolate the EPID response with MU setting by first determining that the EPID response is stable for high MU settings and use these high settings for the FF to remove the effect of this. The change in EPID response with MU setting can then be more easily studied.

The EPIDs are often used for dosimetry without any additional buildup placed on the detector. The measurements of off-axis EPID response with MU setting for 6 MV were repeated for EPID-B with no build-up on the EPID and compared with the measurements with 0.5 cm build-up. These were generally very similar, particularly in the cross-plane direction, with the profiles for above 10 MU being virtually identical. Differences were greater in the in-plane direction although the major trends were still observed, which may be due to random fluctuations in the response. The results obtained here are still applicable for the use of the EPID without additional build-up.

The beam dose rate can differ when images are being acquired with the EPID from normal linac operation. The Varian system has a signal that is sent to the dose-rate servo system when EPID image acquisition is initiated to "freeze" the dose rate once it has reached a certain level. To rule out the possibility that the operation of the EPID somehow affects the beam profile off-axis ratio, ion-chamber measurements were also repeated with the EPID acquiring images during the irradiation. Ion-chamber measurements at 1.5 cm depth in solid water at 100 cm SSD were made at central axis and 15 cm off-axis in the cross-plane direction. The EPID was placed at 125 cm below the couch supporting the solid water phantom and the field size was 24×33 cm^2. Monitor unit settings from 1 to 200 were used and the readings recorded to obtain the off-axis ratio as a function of MU. EPID integrated images were acquired during each irradiation. The ion-chamber off-axis ratios were consistent with MU setting as found previously, with only 0.14% standard deviation of the ratios. There was no trend apparent with decreasing MU except a very slight reduction in the ratios for the small MU settings of 1, 2, and 5.

For the newer EPID-B the EPID profiles are relatively smooth, but the response increases with off-axis distance for low MU settings, whereas for the older EPID-A the profiles for smaller MU settings are nonuniform or "lumpy," and the profile is not symmetric in the in-plane direction. While the degree of nonuniformity of the EPID profile varies with MU setting, it is relatively stable and reproducible for each MU setting. An interesting feature is that the profile nonuniformity is not readily apparent at 18 MV energy where the profiles are smoother. This effect is not due to FF calibration as this does not remove the nonuniformity, except for the situation where the MU setting used for the FF is identical to the MU for the image. Further work is required to examine the effect of radiation damage on the dosimetric response of these detectors.

The movie-loop acquisition of equal frame images showed that the images near the start of the irradiation exhibit the increased off-axis response, whereas the images at the end of the irradiation are more uniform. These results suggest that the effect is related to beam on time rather than an EPID imaging time effect. If the effect was simply related to the number of image frames, then no difference in these movie-loop images would be expected. For the images shown in Figs. 3 and 4, then the shorter MU images will show the effect, and it will reduce in importance for the larger MU images, as these contain more frames acquired later in the irradiation.

The offset detector images also clearly showed that the EPID response is related to the position within the beam rather than the position of an EPID detector. If the off-axis increase was related to a pixel sensitivity gradient due for example to the manufacturing process, then offsetting the detector would not change the position of the response in the pixel matrix. The introduction of filtering material also shows a decrease in the off-axis response for the shorter MU irradiations. The 8 cm of perspex and 1.6 cm of Cu will be sufficient to filter the lower energy photons and give a relatively uniform beam spectrum incident on the EPID. While the beam profile will obviously be different for these images from an unattenuated beam, they were normalized to the 200 MU image to remove this effect. There will also be scatter from the filtering material. This was minimized by keeping an air gap of 22.5 cm to the EPID. A uniform scatter contribution of 50% was also subtracted from the images to ensure that the increase in signal due to scatter was not masking the increase in profiles. There was no apparent change in the profiles when this was done.

A possibility is that this effect may be related to changes of the beam spectrum with beam-on time. However, the ion-chamber measurements of beam quality did not show that these spectrum changes occur, and without specialized spectrum measurement equipment it may not be possible to confirm this.

These measurements were performed for large open fields, and the results are likely to be different from these for IMRT fields with varying dose components of open and MLC transmitted beams. The results performed with filtration material showed a much reduced change in off-axis response with MU setting. Therefore for IMRT fields this effect would be expected to reduce with increasing component of MLC transmitted dose to a pixel.

V. CONCLUSIONS

The EPID dose response was assessed at both central axis and at off-axis points relative to the central axis. The EPID response was found to increase off-axis relative to central axis with small MU settings, with up to 5% difference in response at 20 cm off-axis for an older EPID and within 2% for a newer EPID. Experiments performed to investigate the cause of the nonuniformity of response showed that it depends on the distance of the pixel from central axis, was present for images acquired closer to beam on, and was much reduced when sufficient beam filtering phantom thickness was present. The exact cause of the response at this time remains inconclusive, but is unlikely to be a significant problem for IMRT dosimetry with this manufacturers equipment where MU settings of 100 to 300 are common for IMRT fields, provided that the EPID is not exhibiting large changes in off-axis response due to radiation damage.

ACKNOWLEDGMENTS

The author gratefully acknowledges the assistance of Dr. Boyd McCurdy of Cancer Care Manitoba, Dr. Marcus Wendling of the Netherlands Cancer Institute, and Joan Hatton of the Newcastle Mater Misericordiae Hospital with this work.

[a]Electronic mail: peter.greer@mater.health.nsw.gov.au; Telephone: 61 2 4921 1510; Fax: 61 2 4921 1138.
[1]P. Munro and D. C. Bouius, "X-ray quantum limited portal imaging using amorphous silicon flat-panel arrays," Med. Phys. **25**, 689–702 (1998).
[2]Y. El-Mohri, L. E. Antonuk, J. Yorkston, K. W. Jee, M. Maolinbay, K. L. Lam, and J. H. Siewerdsen, "Relative dosimetry using active matrix flat-panel imager (AMFPI) technology," Med. Phys. **26**, 1530–1541 (1999).
[3]B. M. C. McCurdy, K. B. Luchka, and S. Pistorius, "Dosimetric investigation and portal dose image prediction using an amorphous silicon electronic portal imaging device," Med. Phys. **28**, 911–924 (2001).
[4]P. B. Greer and C. C. Popescu, "Dosimetric properties of an amorphous silicon electronic portal imaging device for verification of dynamic intensity modulated radiation therapy," Med. Phys. **30**, 1618–1627 (2003).
[5]G. V. Menon and R. S. Sloboda, "Compensator quality control with an

amorphous silicon EPID," Med. Phys. **30**, 1816–1824 (2003).
[6]A. van Esch, T. Depuydt, and D. P. Huyskens, "The use of an *a*Si-based EPID for routine absolute dosimetric per-treatment verification of dynamic IMRT fields," Radiother. Oncol. **71**, 223–234 (2004).
[7]L. N. McDermott, R. J. W. Louwe, J.-J. Sonke, M. B. van Herk, and B. J. Mijnheer, "Dose-response and ghosting effects of an amorphous silicon electronic portal imaging device," Med. Phys. **31**, 285–295 (2004).
[8]P. Winkler, A. Hefner, and D. Georg, "Dose-response characteristics of an amorphous silicon EPID," Med. Phys. **32**, 3095–3105 (2005).
[9]L. N. McDermott, S. M. J. J. G. Nijsten, J.-J. Sonke, M. Partridge, M. van Herk, and B. J. Mijnheer, "Comparison of ghosting effects for three commercial *a*-Si EPIDs," Med. Phys. **33**, 2448–2451 (2006).
[10]P. W. Chin and D. G. Lewis, "The Varian *a*S500 EPID as a dosemeter: preliminary investigations," in *Proceedings of the 8th International Workshop on Electronic Portal Imaging*, Brighton, UK (June, 2004).
[11]G. Budgell, Q. Zhang, R. Trouncer, and R. Mackay, "Improving IMRT quality control efficiency using an amorphous silicon electronic portal imager," Med. Phys. **32**, 3267–3278 (2005).
[12]C. Kirkby and R. Sloboda, "Consequences of the spectral response of an *a*-Si EPID and implications for dosimetric calibration," Med. Phys. **32**, 2649–2658 (2005).
[13]P. B. Greer, "Correction of pixel sensitivity variation and off-axis response for amorphous silicon EPID dosimetry," Med. Phys. **32**, 3558–3568 (2005).
[14]W. Li, J. V. Siebers, and J. A. Moore, "Using fluence separation to account for energy spectra dependence in computing dosimetric *a*-Si EPID images for IMRT fields," Med. Phys. **33**, 4468–4480 (2006).
[15]L. Parent, J. Seco, P. M. Evans, A. Fielding, and D. R. Dance, "Monte-Carlo modelling of *a*-Si EPID response: The effect of spectral variations with field size and position," Med. Phys. **33**, 4527–4540 (2006).
[16]L. Ko, J. O. Kim, and J. V. Siebers, "Investigation of the optimal backscatter for an *a*Si electronic portal imaging device," Phys. Med. Biol. **49**, 1723–1738 (2004).